Significant modulation of electrical spin accumulation by efficient thermal spin injection

Shaojie Hu[1] and Takashi Kimura[2,3,4,*]

[1]*Graduate School of Information Science and Electrical Engineering, Kyushu University, 744 Motooka, Fukuoka, 819-0395, Japan*

[2]*Department of Physics, Kyushu University, 6-10-1 Hakozaki, Fukuoka, 812-8581, Japan*

[3]*Research Center for Quantum Nano-Spin Sciences, Kyushu University, 6-10-1 Hakozaki, Fukuoka, 812-8581, Japan*

[4]*CREST, Japan Science and Technology Agency, Sanbancho, Tokyo 102-0075, Japan*

(Received 24 July 2014; revised manuscript received 14 September 2014; published 14 October 2014)

We have investigated the dc bias current dependence of the nonlocal spin valve signal in CoFeAl/Cu lateral spin valves. The spin signal is found to increase monotonically with the bias current. Surprisingly, the modulation amplitude from −1 mA to 1 mA exceeds 30 percent of the spin signal at low bias current. From the analysis based on the one-dimensional spin diffusion model and considering the bias-current heating effect, we find that the contribution of the thermal spin injection is much larger than the influence of the reduction of the spin diffusion length due to the Joule heating. We also show that the second harmonic lock-in signal precisely extracts the contribution of the thermal spin injection from the mixed spin signal.

DOI: 10.1103/PhysRevB.90.134412 PACS number(s): 75.76.+j, 66.70.Df

Manipulation of spin current is a central issue in the operation of spintronic devices, because the spin current plays a key role in spin-dependent transports [1–3] and spin-transfer switching [4,5]. Recently, a laterally-configured ferromagnet(FM)/nonferromagnet(NM) hybrid nanostructure, so-called lateral spin valves (LSV), has received considerable attention because the multiterminal configuration can realize flexible and functional device geometries compared with conventional vertical stack structures [6–10]. This enables us to create a pure spin current, which means a flow of angle momentum without accompanying charge current. However, the generation efficiency of the pure spin current is quite low, giving rise to a serious obstacle in the practical application. Recently, the generation efficiency was demonstrated to be improved significantly by employing a spin injector consisting of Heusler compounds [11–13].

As another approach for creating the pure spin current, a heat utilization, which opens the emerging field of spin caloritronics [14], has been paid considerable attention. Various mechanisms for generating spin current utilizing heat such as spin Seebeck effect [15], spin dependent Seebeck effect [16,17], Seebeck spin tunneling effect [18], and spin heat accumulation [19,20] have been demonstrated in different device structures. However, the generation efficiencies were smaller than that by electrical means, indicating quite far from the practical application. Recently, we have shown that the thermal spin injection efficiency was dramatically enhanced by using a CoFeAl injector because of a sign reversal of the Seebeck coefficient between the up and down spins [21]. This demonstration may open an avenue for the utilization of the spin current in the nanoelectronic devices. In this paper, for further enhancement of the spin signal and generation efficiency of the spin current, we experimentally investigated the bias current dependence of the nonlocal spin valve signal in CoFeAl/Cu lateral spin valves. By mixing the thermal spin injection on the electrical spin injection, we demonstrate a large directional modulation of the generation efficiency of the spin current.

*t-kimu@phys.kyushu-u.ac.jp

The CoFeAl/Cu LSVs were fabricated by two-steps lift-off processes based on the electron beam lithography. Figure 1 shows a scanning electron microscope (SEM) image of the typical device for the present study. First, two ferromagnetic CoFeAl (CFA) wires, 30 nm in thickness and 120 nm in width, were fabricated by electron-beam evaporation under ultra-high vacuum ($\sim 10^{-8}$ Pa). After that, a nonmagnetic Cu channel with the thickness of 160 nm and the width of 120 nm was deposited by Joule-heating evaporation. Here, the surface of CFA was well cleaned by using low-power Ar^+ ion milling.

The spin transports under the electrical and thermal spin injections were evaluated by nonlocal spin detection technique. The spin injection was performed by flowing the current from the $CFA_{inj.}$ to the Cu channel. Here, the current consists of a small ac current ($I_{ac} = \sqrt{2} I_0 \sin(\omega t)$) and the dc bias current I_{dc}. Note that the electron flowing from the Cu to the $CFA_{inj.}$ is defined as positive sign of I_{dc}. The accumulated spins due to the spin injection were detected by measuring the electrical voltage between $CFA_{det.}$ and Cu channel. Here, the voltages with first and second harmonic frequency were separately detected by using lock-in amplifier. Since a large current induces a nonlinear voltage, the detected voltage includes higher-order terms, namely $V = R_1 I + R_2 I^2 + R_3 I^3 + R_4 I^4 + \ldots$. The contribution of the spin-dependent term can be extracted from the voltage difference between the parallel and antiparallel states, namely,

$$V_S \equiv V_P - V_{AP} = R_{S1} I + R_{S2} I^2 + R_{S3} I^3 + R_{S4} I^4 + \ldots, \quad (1)$$

where R_{Si} is the spin dependent component defined by the difference between the parallel and antiparallel state, $R_{iP} - R_{iAP}$.

First, we evaluated the linear component R_{S1} by measuring V_S induced by a small ac current, in which higher-order effects can be negligible. Here, we adapt 140 μA as a root mean square value of the ac current I_0 because the linear variations of the spin and background voltages were clearly confirmed at $I_0 \leqslant 140$ μA. Figure 1(b) shows a typical field dependence of a room-temperature nonlocal spin signal R_S. The value of R_S for the present CFA/Cu LSV with the interval of 300 nm is over 6 mΩ, which is much larger than those in Py/Cu LSV with

the same device dimension. We also define the background signal R_B as $R_{1P} + R_{1AP}$, which is the normalized average voltage. The origin of R_B is understood by the Peltier and Seebeck coupling [22] and/or the inhomogeneous distribution of current density [9,23]. Figure 1(c) shows R_S as a function of the distance L. The results are well reproduced by the one-dimensional spin diffusion model with transparent interfaces, given by the following equation [24,25]:

$$R_S = \frac{P_F^2 R_{SF}^2 R_{SN}}{2R_{SF}(R_{SF} + R_{SN})(\cosh(L/\lambda_N) + \sinh(L/\lambda_N)) + R_{SN}^2 \sinh(L/\lambda_N)}. \quad (2)$$

Here, R_{SF} and R_{SN} are the spin resistances for ferromagnet and nonmagnet, respectively. P_F and λ_N are the spin polarization for the ferromagnet and spin diffusion length for the nonmagnet, respectively. From the fitting of Eq. (2) with assuming the spin diffusion length of 2 nm for CFA, the spin polarization for our CFA is estimated as 0.62. This indicates that the large spin signal obtained in the CFA/Cu LSVs is attributed to the efficient generation and detection of the spin current originating from the high spin polarization.

Then, we systematically investigated the first harmonic spin signal R_S^{1f} under the DC bias current as shown in Figs. 2(a)–2(c). Here, we define the first harmonic spin signal R_S^{1f} as $\Delta V_S^{1f}/I_0 = (V_P^{1f} - V_{AP}^{1f})/I_0$, which is the normalized voltage difference between parallel and antiparallel states. R_S^{1f} shows the largest value of 7.66 mΩ at $I_{dc} = 1$ mA while it takes the smallest value of 5.28 mΩ at $I_{dc} = -1$ mA. Figure 2(d) shows R_S^{1f} as a function of I_{dc}. Overall signal change from −1 mA to 1mA is 2.38 mΩ, which exceeds 30% of R_S^{1f} at $I_{dc} = 0$. Thus, the spin signal R_S^{1f} is found to be strongly modulated by I_{dc}. Especially, the enhancement of the spin signal under the positive high bias current is an attractive characteristic from the viewpoint of the spin injection.

To understand the modulation effect quantitatively, we consider higher order effects in the first harmonic voltages under the ac and dc currents $I = I_{ac} + I_{dc}$. If we consider the second, third, and fourth order effects in Eq. (1), the first harmonic spin-dependent voltage ΔV_S^{1f} and spin signal $R_S^{1f} \equiv \Delta V_S^{1f}/I_0$ are obtained by the following equations [16]:

$$\Delta V_S^{1f} = \left(R_{S1} + 2R_{S2}I_{dc} + 3R_{S3}I_{dc}^2 + 4R_{S4}I_{dc}^3\right)I_0 \quad (3)$$

$$R_S^{1f} = R_{S1} + 2R_{S2}I_{dc} + 3R_{S3}I_{dc}^2 + 4R_{S4}I_{dc}^3. \quad (4)$$

Importantly, the dc current dependence of R_S^{1f} observed in Fig. 2(d) is well reproduced by Eq. (4) with $R_{S1} = 6.96$ mΩ, $R_{S2} = 0.60$ mΩ/mA, $R_{S3} = -0.16$ mΩ/mA^2, and $R_{S4} = -0.02$ mΩ/mA^3. Note that R_{S2} and R_{S3} are the coefficients for I_{dc} and I_{dc}^2 in Eq. (4). Therefore, when $|I_{dc}|$ is less than 1 mA, ΔR_S is almost linearly proportional to I_{dc} in the CFA/Cu LSV.

We then discuss the physical meanings of the higher order effects, R_{S2}, R_{S3}, and R_{S4}. By taking into account the contribution of the thermal spin injection under the temperature gradient ∇T, Eq. (2) can be expanded as follows [16,21]:

$$V_S \approx \frac{P_F(P_F I + \lambda_F S_S \nabla T/R_{SF})R_{SF}^2}{R_{SN}\sinh(L/\lambda_N)}. \quad (5)$$

Here, the first term of the denominator in Eq.(2) is neglected by considering the condition $R_{SN} \gg R_{SF}$. S_S is the spin-dependent Seebeck coefficient for CFA. We also consider the influence of the reduction of λ_N due to the increase of the dc bias current by using the following relationship $\lambda_N = \lambda_{N0} - \Delta\lambda_N$. Here, λ_{N0} is the spin diffusion length for the Cu at room temperature and $\Delta\lambda_N$ is its change due to the temperature rising. By using the approximation $\frac{L}{\lambda_{N0}-\Delta\lambda_N} \approx \frac{L}{\lambda_{N0}}(1 + \frac{\Delta\lambda_N}{\lambda_{N0}})$

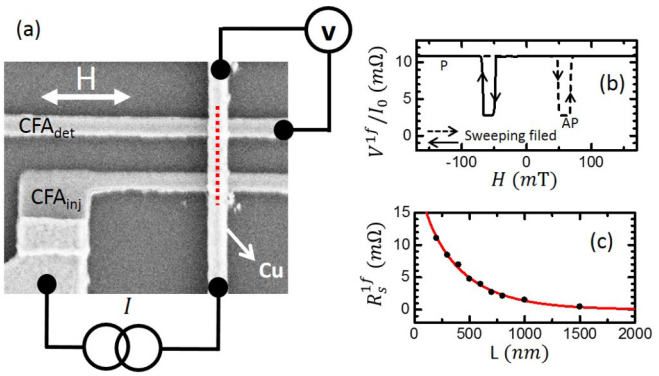

FIG. 1. (Color online) (a) SEM image of the fabricated LSV device consisting of two CoFeAl wires and a single Cu channel strip. (b) Representative nonlocal spin signal observed in CFA/Cu LSV under the ac current of $I_0 = 140\mu$A without the dc current. The dash and solid curves correspond to forward and backward field sweeps, respectively. (c) First harmonic spin signal without dc current as a function of interval distance L. The solid red curve is obtained by fitting Eq. (2) to the experimental points.

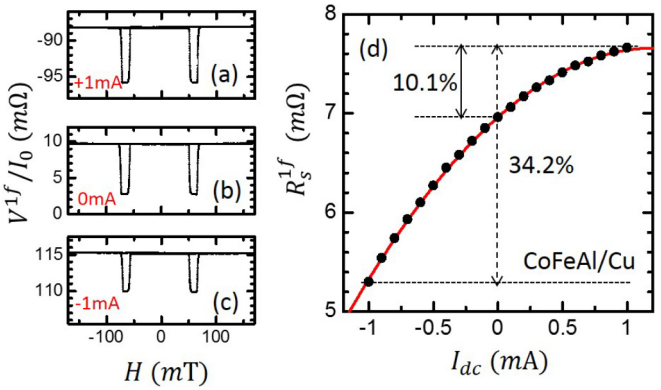

FIG. 2. (Color online) Field dependence of the first harmonic signal with the dc bias currents (a) +1 mA, (b) 0 mA, and (c) −1 mA. (d) First harmonic spin signal R_S^{1f} as a function of dc bias current (I_{dc}) for the CFA/Cu LSV with the interval distance 400 nm. The solid line corresponds to the fitting curve based on Eq. (4).

with Taylor series of $\sinh x$, Eq. (5) can be extended to

$$V_S \approx \frac{R_{SF}^2}{R_{SN}} P_F (P_F I + \lambda_F S_S \nabla T / R_{SF}) \times \left(\frac{1}{\sinh(L/\lambda_{N0})} - \frac{\cosh(L/\lambda_{N0})}{\sinh^2(L/\lambda_{N0})} \frac{L}{\lambda_{N0}} \frac{\Delta\lambda_N}{\lambda_{N0}} \right). \quad (6)$$

Since the temperature change due to the dc bias current is caused by Joule heating, it is natural to assume $\nabla T = aI^2$, where a is the constant conversion factor. $\Delta\lambda_N$ is also caused by the temperature change due to the Joule heating. In the temperature range above 50 K, the spin diffusion length monotonically decreases with increasing the temperature [26–28]. Therefore, when the temperature variation ΔT due to the Joule heating is much smaller than the base temperature T_0, in the present case 300 K, we obtain $\Delta\lambda_N \propto \Delta T$ from the Taylor series approximation. Since the temperature variation is proportional to the Joule heating, we also obtain $\Delta\lambda_N = bI^2$, where b is the constant conversion factor.

Then, the first harmonic spin signal R_S^{1f} can be expressed by the following equation:

$$R_S = \frac{V_S}{I} \approx \frac{P_F R_{SF}^2}{R_{SN} \sinh(L/\lambda_{N0})} \left(P_F + \frac{a\lambda_F S_S}{R_{SF}} I - \frac{bL \coth(L/\lambda_{N0})}{\lambda_{N0}^2} \left(P_F I^2 + \frac{a\lambda_F S_S}{R_{SF}} I^3 \right) \right). \quad (7)$$

From the comparison between Eqs. (4) and (7), The second, third, and fourth resistances R_{S2}, R_{S3}, and R_{S4} are found to stem from the thermal spin injection, influence of the reduction of the spin diffusion length of Cu on the electrical spin injection and that on the thermal spin injection, respectively. Especially, the comparisons of the first and second terms yield the following relationship:

$$\frac{2R_{S2}}{R_{S1}} = \frac{a\lambda_F S_S}{P_F R_{SF}}. \quad (8)$$

Here, R_{S1} can be given by the first harmonic spin signal without the dc current. Since a can be calculated as 0.15 K nm^{-1} mA^{-2} from COMSOL simulation [29,30], we obtain $S_S = -72.2\ \mu$V/K.

For further confirmation of the influence of the thermal spin injection, we also evaluated the second harmonic voltage in the same measurement configuration. This approach enables us to exclude the influence of the electrical spin injection, and directly obtain R_{S2} from the signal. As shown in Figs. 3(a)–3(c), the clear spin signals can be seen also in the second harmonic voltage under various AC bias currents. Since the detected second harmonic voltage is given by $R_{S2}I_0^2/\sqrt{2}$, R_{S2} can be calculated as 0.6 mΩ/mA, which is exactly the same as the value obtained in the results of fitting DC bias current. The base resistance is also found to be reproduced by the same manner.

For the comparison, we also evaluated R_S^{1f} for various dc current injection for the Py/Cu LSV with a similar device dimension. Figure 4 shows R_S^{1f} as a function of I_{dc} with a representative spin signal for $I_{dc} = 0$. As can be seen in Fig. 4, R_S^{1f} parabolically reduces with increasing I_{dc} and it is difficult to see a monotonic tendency originating from the thermal spin injection. From the fitting curve using Eq. (4), we obtain $R_{S1} =$ 0.79 mΩ, $R_{S2} = 0.0079$ mΩ/mA, $R_{S3} = -0.016$ mΩ/mA^2, and $R_{S4} = -0.00024$ mΩ/mA^3. This enables us to estimate $S_S = -2.5\ \mu$V/K with assuming $a = 0.12$ K nm^{-1} mA^{-2} for the Py/Cu LSV structure. The value is much smaller than that for the CFA. This means that the variation of the spin signal R_S is dominated by $R_{S3}I_{dc}^2$, resulting in the parabolic reduction of the spin signal.

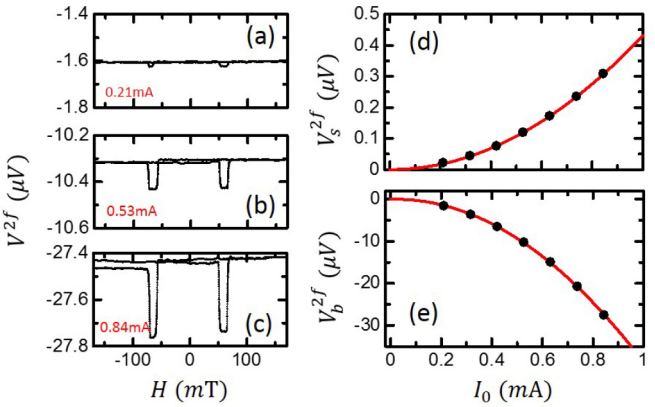

FIG. 3. (Color online) Field dependence of the second harmonic voltage for the ac currents (a) 0.21 mA, (b) 0.53 mA, and (c) 0.84 mA. (d) Second harmonic spin voltage $V_S^{2f} = V_P^{2f} - V_{AP}^{2f}$ and (e) base voltage of second harmonic $V_B^{2f} = (V_P^{2f} + V_{AP}^{2f})/2$ as a function of AC bias current (I_0). The solid red curves represent the fitting parabolic curve.

Thus, the spin dependent Seebeck coefficient for CFA is found to be much larger than that for the Py. Especially, 10 percent enhancement of the spin signal under high bias current is a great advantage for generating the large spin current. By extending the present mixing technique, in principle, it is possible that the generation efficiency of the electrical spin injection exceeds 100 percent. In addition, we know that in the Py/Cu LSV, the spin signal is significantly smeared out by anomalous Nernst-Ettingshausen effect and anisotropic magneto-Seebeck effect [31–33]. Negligible spurious signals in the nonlocal signal under high-bias current for CFA/Cu LSVs is another important advantage.

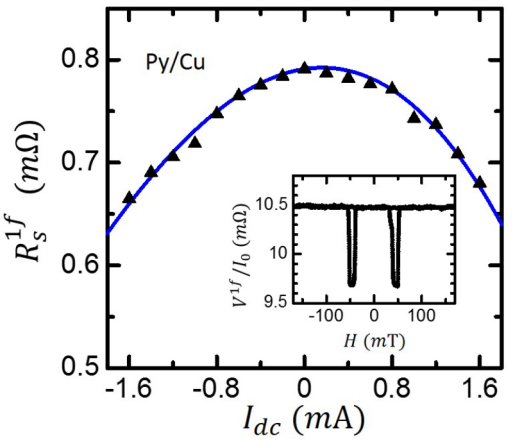

FIG. 4. (Color online) First harmonic spin signal R_S^{1f} as a function of dc bias current (I_{dc}) for the Py/Cu LSV. The solid line corresponds to the fitting curve based on Eq. (4). The inset shows the representative field dependence of the spin signal for ($I_{dc} = 0$).

This work is partially supported by KAKENHI(25220605), CANON Foundation, and CREST. The author (Shaojie Hu) acknowledges the China Scholarship Council (CSC) for Young Scientists.

[1] I. Žutić, J. Fabian, and S. Das Sarma, Rev. Mod. Phys. **76**, 323 (2004).
[2] *Concepts in Spin Electronics*, edited by S. Maekawa (Oxford University Press, Oxford, UK, 2006).
[3] *Handbook of Spin Transport and Magnetism*, edited by Evgeny Y. Tsymbal and Igor Zutic (CRC, Boca Raton, US, 2011).
[4] E. B. Myers, D. C. Ralph, J. A. Katine, R. N. Louie, and R. A. Buhrman, Science **285**, 867 (1999).
[5] J. A. Katine, F. J. Albert, R. A. Buhrman, E. B. Myers, and D. C. Ralph, Phys. Rev. Lett. **84**, 3149 (2000).
[6] M. Johnson and R. H. Silsbee, Phys. Rev. Lett. **55**, 1790 (1985).
[7] F. J. Jedema, A. T. Filip, and B. J. van Wees, Nature (London) **410**, 345 (2001).
[8] S. O. Valenzuela, Int. J. Mod. Phys. B **23**, 2413 (2009).
[9] T. Kimura and Y. Otani, J. Phys.: Condens. Matter **19**, 165216 (2007).
[10] A. Hoffmann, Phys. Stat. Sol. (C) **4**, 4236 (2007).
[11] T. Kimura, N. Hashimoto, S. Yamada, M. Miyao, and K. Hamaya, NPG Asia Mater. **4**, e13 (2012).
[12] K. Hamaya, N. Hashimoto, S. Oki, S. Yamada, M. Miyao, and T. Kimura, Phys. Rev. B **85**, 100404(R) (2012).
[13] Y. K. Takahashi, S. Kasai, S. Hirayama, S. Mitani, and K. Hono, Appl. Phys. Lett. **100**, 052405 (2012).
[14] G. E. W. Bauer, E. Saitoh, and B. J. van Wees, Nat. Mater. **11**, 391 (2012).
[15] K. Uchida, S. Takahashi, K. Harii, J. Ieda, W. Koshibae, K. Ando, S. Maekawa, and E. Saitoh, Nature (London) **455**, 778 (2008).
[16] A. Slachter, F. L. Bakker, J.-P. Adam, and B. J. van Wees, Nat. Phys. **6**, 879 (2010).
[17] M. Erekhinsky, F. Casanova, I. K. Schuller, and A. Sharoni, Appl. Phys. Lett. **100**, 212401 (2012).
[18] J.-C. Le Breton, S. Sharma, H. Saito, S. Yuasa, and R. Jansen, Nature (London) **475**, 82 (2011).
[19] I. J. Vera-Marun, B. J. van Wees, and R. Jansen, Phys. Rev. Lett. **112**, 056602 (2014).
[20] F. K. Dejene, J. Flipse, G. E. W. Bauer, and B. J. van Wees, Nat. Phys. **9**, 636 (2013).
[21] S. Hu, H. Itoh, and T. Kimura, NPG Asia Mater. **6**, e127 (2014).
[22] F. L. Bakker, A. Slachter, J.-P. Adam, and B. J. van Wees, Phys. Rev. Lett. **105**, 136601 (2010).
[23] M. Johnson and R. H. Silsbee, Phys. Rev. B **76**, 153107 (2007).
[24] S. Takahashi and S. Maekawa, Phys. Rev. B **67**, 052409 (2003).
[25] T. Kimura, J. Hamrle, and Y. Otani, Phys. Rev. B **72**, 014461 (2005).
[26] T. Kimura, T. Sato, and Y. Otani, Phys. Rev. Lett. **100**, 066602 (2008).
[27] G. Mihajlović, J. E. Pearson, S. D. Bader, and A. Hoffmann, Phys. Rev. Lett. **104**, 237202 (2010).
[28] E. Villamor, M. Isasa, L. E. Hueso, and F. Casanova, Phys. Rev. B **88**, 184411 (2013).
[29] S. R. Bakaul, S. Hu, and T. Kimura, Appl. Phys. A **111**, 355 (2012).
[30] C. Mu, S. Hu, J. Wang, and T. Kimura, Appl. Phys. Lett. **103**, 132408 (2013).
[31] S. Hu and T. Kimura, Phys. Rev. B **87**, 014424 (2013).
[32] A. D. Avery, M. R. Pufall, and B. L. Zink, Phys. Rev. B **86**, 184408 (2012).
[33] A. D. Avery, M. R. Pufall, and B. L. Zink, Phys. Rev. Lett. **109**, 196602 (2012).